Dissociation of ground and n* states of CF3Cl using multireference configuration interaction with singles and doubles and with multireference average quadratic coupled cluster extensivity corrections

Juracy R. Lucena, Elizete Ventura, Silmar A. do Monte, Regiane C. Araújo, Mozart N. Ramos et al.

Citation: J. Chem. Phys. **127**, 164320 (2007); doi: 10.1063/1.2800020
View online: http://dx.doi.org/10.1063/1.2800020
View Table of Contents: http://jcp.aip.org/resource/1/JCPSA6/v127/i16
Published by the American Institute of Physics.

Dissociation of ground and $n\sigma^*$ states of CF_3Cl using multireference configuration interaction with singles and doubles and with multireference average quadratic coupled cluster extensivity corrections

Juracy R. Lucena, Jr.,[a] Elizete Ventura,[b),c)] Silmar A. do Monte,[b),d)] and Regiane C. M. U. Araújo
Departamento de Química, CCEN, Universidade Federal da Paraíba, João Pessoa, Paraíba 58036-300 Brazil

Mozart N. Ramos
Departamento de Química Fundamental, Universidade Federal de Pernambuco, Recife, Pernambuco 50739-901, Brazil

Rui Fausto
Department of Chemistry (CQC), University of Coimbra, 3004-535 Coimbra, Portugal

(Received 14 March 2007; accepted 25 September 2007; published online 30 October 2007)

Extended complete active space self-consistent field (CASSCF), multireference configuration interaction with singles and doubles (MR-CISD), and multireference average quadratic coupled cluster (MR-AQCC) calculations have been performed on the ground (S_0) and first excited ($n\sigma^*, S_1$) states of the CF_3Cl molecule. Full geometry optimizations have been carried out for S_0 as well as "relaxed" potential energy calculations for both states, along the C–Cl bond distance. Vertical excitation energies ($\Delta E_{\text{vertical}}$), dissociation energies (ΔE_{diss}), dissociation enthalpies (ΔH_{diss}), and the oscillator strength (f) have also been computed. Basis set effects, basis set superposition error (BSSE), and spin-orbit and size-extensivity corrections have also been considered. The general agreement between theoretical and available experimental results is very good. The best results for the equilibrium geometrical parameters of S_0 (at MR-AQCC/aug-cc-pVTZ+d level) are 1.762 and 1.323 Å, for the C–Cl and C–F bond distances, respectively, while the corresponding experimental values are 1.751 and 1.328 Å. The $\angle_{\text{ClCF}}$ and $\angle_{\text{FCF}}$ bond angles are in excellent agreement with the corresponding experimental values (110.3° and 108.6°). The best calculated values for $\Delta E_{\text{vertical}}$, ΔH_{diss}, and f are 7.63 eV [at the MR-AQCC/aug-cc-pV(T+d)Z level], 3.59 eV [MR-AQCC/aug-cc-pV(T+d)Z level+spin-orbit and BSSE corrections], and 2.74×10^{-3} (MR-CISD/cc-pVTZ), in comparison with the corresponding experimental values of 7.7±0.1 eV, 3.68 eV, and $3.12\times10^{-3}\pm2.50\times10^{-4}$. The results concerning the potential energy curves for S_0 and S_1 show a tendency toward the nonoccurrence of crossing between these two states (in the intermediate region along the C–Cl coordinate), as the basis set size increases. Such tendency is accompanied by a decreasing well depth for the S_1 state. Dynamic electronic correlation (especially at the MR-AQCC level) is also an important factor toward an absence of crossing along the C–Cl coordinate. Further investigations of a possible crossing using gradient driven techniques (at CASSCF and MR-CISD levels) seem to confirm its absence. © *2007 American Institute of Physics*. [DOI: 10.1063/1.2800020]

I. INTRODUCTION

The role of clorofluorcarbons (CFCs) as depleting agents of Earth's ozone layer in the stratosphere has been well established,[1–3] being nowadays a subject of great concern.[4–7] CFC action as ozone depleters is connected to their photodissociation, which yields chlorine radicals (Cl·) that catalyze the cleavage of ozone molecules through chain reactions.[1] Therefore, the study of the photochemistry of such molecules is crucial in order to get a deeper insight into their mechanism of action.

The energies of the lowest electronically excited states of CFCs, obtained from absorption spectra, lay in the range of 6.5–9.7 eV.[8–10] Between approximately 6.5 and 8.8 eV the absorption spectra can be characterized by very broad, weak bands corresponding to transitions from the Cl lone pairs (n,3p) to the antibonding C–Cl σ^* orbitals. Such transitions are expected to be dissociative, thus leading to formation of Cl· and chlorofluoromethyl radicals. The $n\sigma^*$ transitions in CF_3Cl,[11,12] CF_2Cl_2,[11] $CFCl_3$,[11] CCl_4,[13] and CHF_2Cl (Ref. 14) contain a significant quadrupole component that resembles that of an atomic $p\rightarrow p$ transition in a Cl atom, which explains its low intensity, despite its dipole-allowed

[a)]Permanent address: Departamento de Química, Universidade Estadual da Paraíba, Campina Grande, Paraíba 58101-001, Brazil.
[b)]Authors to whom correspondence should be addressed.
[c)]Tel.: +55 88 3216 7590. FAX: +55 83 3216 7437. Electronic mail: elizete@quimica.ufpb.br
[d)]Electronic mail: silmar@quimica.ufpb.br

nature. Much stronger and sharper bands lay between approximately 8.9 and 9.7 eV. These bands have been assigned to $n \rightarrow (4s, 4p, 4d)$ Rydberg transitions. The lack of well-defined vibrational structure in these Rydberg absorption bands suggests the involvement of dissociative or rapidly predissociated upper states.[15] The photodissociation of CF_3X (where X=H,Cl,Br) can be monitored from emission spectra of the $CF_3\cdot$ radical.[16]

In the case of CF_3Cl, the $n\sigma^*$ band has its maximum at about 7.7 eV,[12] while the Rydberg band maximum is found at about 9.7 eV.[8] Despite the lower intensity of the $n\sigma^*$ transition (as compared with the Rydberg series), there are two important and still open questions that can be expected to be successfully addressed by high-level quantum chemistry calculations: (i) Is the $n\sigma^*$ state repulsive or attractive (along the C–Cl coordinate)? If it is attractive, what is the associated well depth? and (ii) is there any crossing of this state with the ground state in the intermediate C–Cl region? A positive answer to the first question would possibly imply a greater lifetime for the $n\sigma^*$ state, when compared to the situation in which this state is repulsive. A positive answer to the second question would imply a possible recombination channel via the $n\sigma^*$ state. Ying *et al.*[12] performed potential energy calculations along the C–Cl bond distance for the ground (S_0) and $n\sigma^*$ (S_1) states of CF_3Cl, at the *ab initio* configuration interaction singles (CIS) level with the 6-31G and 6-31++G** basis sets. These authors obtained dissociation energies of about 8.1 and 2 eV for the S_0 and S_1 states, respectively. Besides, they also obtained a S_0/S_1 crossing above 0.4 nm, with both basis sets. As we shall show later in this paper, CIS calculations are not accurate enough to describe some features of these two states. For instance, the dissociation energy of S_0 is overestimated, while there are strong indications that the S_1 state is repulsive along the C–Cl coordinate. Another important point is that S_0 and S_1 should cross only upon complete dissociation. Vertical excitation energies are also too high at the CIS level.[12]

More accurate calculations concerning the dissociation energy of CF_3Cl have been performed by Roszak *et al.*, at the MP2/aug-cc-pVTZ level,[17] and a value of 4.014 eV has been obtained. These authors also performed full geometry optimization for this molecule. To the best of our knowledge, there is only one paper dealing with multireference CI calculations on the CF_3Cl molecule.[18] That study was performed only for the ground state and was based on a two electron two orbitals complete active space calculation, (CAS)(2,2), with a cc-pVDZ basis set.[18] In the reported potential energy calculations along the C–Cl bond distance, the CF_3 moiety was held fixed in its asymptotic equilibrium geometry while the Cl atom approaches.[18] Besides, the C–Cl separation range investigated went only from 3.0 to 5.0 Å; such range was selected taking into consideration only the kinetically important region for the dissociation and is certainly not wide enough to allow for reaching the minimum energy along this coordinate.

In general, single-reference CI methods [such as CIS, configuration interaction with singles and doubles (CISD), etc.] can give good results in special cases, but they are most of times not good enough for general surveys of potential energy surfaces. With a proper choice of the active orbitals, a MCSCF wave function[19] has the required flexibility to qualitatively describe the main changes occurring in the wave function character along extended sections of potential energy surfaces. However, results obtained with this method are often not quantitatively satisfactory, since it does not take into account dynamic electron correlation effects. State-averaged multiconfigurational self-consistent field (SA-MCSCF), in combination with multireference configuration interaction with singles and doubles[20] (MR-CISD) methods, provides stable, accurate, and robust procedures for the investigation of entire energy surfaces. State averaging at the MCSCF level provides for a balanced set of molecular orbitals (MOs), and the MR-CISD approach based on such MOs is well suited for simultaneous calculation of a multitude of states. Size-extensivity corrections on the MR-CISD wave function are important and can be computed by means of the generalized Davidson method (MR-CISD+Q),[21,22] which is an *a posteriori* approach or, in a more general and consistent way, by an *a priori* approach, represented by the multireference averaged quadratic coupled cluster (MR-AQCC) method.[23–27] The availability of analytical energy gradients with respect to nuclear coordinates is another major advantage of the MR-CISD and MR-AQCC methods.[28,29]

There are several experimental difficulties concerning characterization of the $n\sigma^*$ state. For instance, the study concerning vacuum ultraviolet (VUV) absorption spectra (200–120 nm) of CF_3Cl, by Doucet *et al.*,[8] reported this transition as a very weak and structureless shoulder of a nearby Rydberg peak, making its precise location very difficult. The *K*-resolved electron energy loss spectroscopy (KEELS) technique has significantly improved the detection of very weak dipole-allowed and dipole-forbidden transitions. (Ref. 12 and references therein). As aforementioned, the $n\sigma^*$ transition corresponds to a very weak quadrupolelike transition, which have been very successfully characterized through the KEELS technique.[12]

The VUV photolysis study of CF_3Cl at 187 nm (6.63 eV) performed by Yen *et al.*,[30] using the technique of time-of-flight mass spectrometry, did not lead to any detectable fragmentation. Besides, the photofragmentation study of Matsumi *et al.*[31] at 193 nm (6.42 eV), in which chlorine atom photofragments are detected by the resonance enhanced multiphoton ionization technique, did not produce any observable chlorine fragmentation, probably because the absorption coefficient is too small. Photofragmentation at 157 nm (~7.9 eV) also yielded no Cl^* ($^2P_{1/2}$) signal. This dissociation channel probably corresponds solely to the $n\sigma^*$ state, since there is no Rydberg character in this state, a fact that is confirmed by our calculations, as observed by comparison between the $\langle \mathbf{r}^2 \rangle$ values [where $\mathbf{r}=(x,y,z)$ vector] of the ground and $n\sigma^*$ states. The main factors which contribute to the fine-structure branching ratios are the absorption coefficient and the probability for the states to jump from one potential curve to another one.[32] Since both ground and $n\sigma^*$ (singlet) states correlate to the chlorine ground state ($^2P_{3/2}$),[31,33] it is not possible to conclude, from this type of experiments, if there is a crossing between these two states in the intermediate region. Thus, since the photodissociation via

the $n\sigma^*$ channel is very difficult to measure, accurate *ab initio* calculations are required if one wants to answer the aforementioned questions. Besides, highly accurate potential energy surfaces may be very helpful in the interpretation of the photochemistry of this type of molecules.[34,35] Therefore, in this study benchmark multireference CI calculations were performed on the ground and $n\sigma^*$ excited states of the CF_3Cl molecule.

II. COMPUTATIONAL DETAILS

The ground state electronic configuration of CF_3Cl may be written as follows, in C_{3v} notation:[36]

inner shells:

$$(\mathrm{Cl}\ 1s)^2(\mathrm{F}\ 1s)^6(\mathrm{C}\ 1s)^2(\mathrm{Cl}\ 2s)^2(\mathrm{Cl}\ 2p)^6,$$

valence shells:

$$(6a_1)^2(3e)^4(7a_1)^2(8a_1)^2(4e)^4(9a_1)^2(5e)^4(6e)^4(1a_2)^2$$

$$(10a_1)^2(7e)^4(11a_1)^0.$$

The $10a_1$, $7e$, and $11a_1$ orbitals correspond to the σ (C–Cl), n (Cl, $3p_x$, $3p_y$), and σ^* (C–Cl) orbitals, respectively. Therefore, the ground state is of A_1 symmetry ($1\ ^1A_1$), while the first excited state is of E symmetry ($1\ ^1E$, doubly degenerate). Upon breakage of the C–Cl bond, the three p orbitals of chlorine atom become degenerate. The $3p_z$ orbital is the one which takes part in the formation of the σ bond and contains more bonding character, while the *quasi-*sp^3 hybrid orbital (which is the one that contains the unpaired electron of the $CF_3\cdot$ radical) contains more σ^* character. Therefore, a "natural" multiconfigurational choice is to include all of them in the active space.

The first step in the calculations here reported consists of a state-averaged MCSCF calculation,[37] where the same weight was given to all states considered. The active space is a CAS (6,4), that is, six electrons are distributed, in all possible ways (consistent with spin and space symmetry) among the σ (C–Cl), (n_x, n_y), and σ^* (C–Cl) orbitals. The same active space was chosen for the construction of the reference configuration state functions (CSFs). C_s symmetry (where the symmetry plane is the xy plane and contains one atom of each type: one F, one C, and one Cl atom) was used in all calculations, and the $1\ ^1A'$, $2\ ^1A'$, and $1\ ^1A''$ states (which correspond to the $1\ ^1A_1$ and $1\ ^1E$ states in C_{3v} symmetry) were considered. The Dunning's correlation consistent cc-pVDZ, aug-cc-pVDZ, cc-pVTZ, and aug-cc-pVTZ basis sets[38,39] were used in these calculations. The cc-pV($n+d$)Z basis set has been proposed in order to give a better description of the dissociation process for molecules containing second row atoms,[40] as compared to the standard cc-pVnZ set. It is formed by adding high-exponent d functions to the ($1d$)-($3d$) sets in the standard correlation consistent basis set, so that the exponents to be used in the final d sets must yield a smooth progression, systematically increasing their coverage of basis function space as n increases.[40] Therefore, this basis set has also been included in the present investigation. The final expansions for the subsequent MR-CISD and MR-AQCC wave functions were built from the reference CSFs and all single and double excitations thereof into all virtual orbitals. The CI dimensions treated in this work vary from about 2.2×10^6 (MR-CISD/cc-pVDZ) to about 53.9×10^6 CSFs (MR-AQCC/aug-cc-pV($T+d$)Z). The aforementioned inner shell orbitals were kept frozen in all post-MCSCF calculations. Several MR-AQCC calculations of $2\ ^1A'$ and $1\ ^1A''$ states showed intruder-state problems, that is, few (maximum three) additional CSFs not included in the reference space obtained an unreasonably large weight. Any weight larger than 1% is considered an intruder state. The importance of inclusion of such CSFs in the reference space is twofold: (i) to speed up the convergence of the eigenvalues/eigenvectores and (ii) to yield smooth potential energy curves. In order to get rid of this problem, these individual CSFs were included in the reference space as well. The COLUMBUS program system was used for all calculations.[41–44] The atomic orbitals (AO) integrals and AO gradient integrals were computed with program modules taken from DALTON.[45]

Full geometry optimizations for the ground state were performed in natural internal coordinates, as defined by Fogarasi *et al.*,[46] using the GDIIS procedure.[47] Based on this initial geometry, "relaxed" potential energy calculations along the C–Cl bond were performed (i.e., for each point, only the C–Cl coordinate was kept frozen, while the remaining degrees of freedom were optimized). The distances considered for the C–Cl bond varied from about 1.8 approximately to 10.8 Å. The first point always corresponded to the C–Cl distance in the ground state optimized geometry. For consistency in computing the dissociation energy, the "supermolecule" approach, with the two considered molecular fragments of 100 Å away from each other, was used instead of the isolated fragments. This approach avoided the possibility of an unequal computation of the size-extensivity correction that would result if one compared the isolated fragments with the bonded molecule.

The basis set superposition error (BSSE) has been considered as well, through the counterpoise (CP) correction.[48,49] Such correction can, in principle, be applied either to the calculation of interaction energies (as dissociation and complexation energies, for instance) or to obtain corrected potential energy surfaces.[50] In the present paper we have only corrected the dissociation energies and enthalpies. The potential energy curve of the ground state could be corrected as well. However, it is not possible to correct the energy of the $n\sigma^*$ state, since the CP correction involves calculations on the isolated fragments, and such state is not defined for the isolated fragments. Since for the purposes of the present paper it does not make sense to correct only one of the two states, such correction has not been performed.

The spin-orbit effect has been considered at CASSCF level only, through the algorithm of Abegg[51] implemented in GAUSSIAN 98. In order to compute the spin-orbit coupling (in the present case between singlet and triplet states), the integrals are calculated in a one-electron approximation involving relativistic terms, and then effective atomic charges are adjusted to reproduce experimental results (e.g., fine-structure splittings[51,55]), avoiding the necessity of calculating the highly time-consuming two-electron spin-orbit integrals. Two electron effects are thus taking into account

TABLE I. Ground state equilibrium geometrical parameters of CF_3Cl (distances in angstroms and angles in degrees). Abbreviations DZP: cc-pVDZ, aug-DZP: aug-cc-pVDZ, TZP: cc-pVTZ, aug-TZP: aug-cc-pVTZ, DZP+*d*: cc-pV(*D*+*d*)*Z*, aug-DZP+*d*: aug-cc-pV(*D*+*d*)*Z*, TZP+*d*: cc-pV(*T*+*d*)*Z*, aug-TZP+*d*: aug-cc-pV(*T*+*d*)*Z*.

		R_{CCl}	R_{CF}	$\angle_{ClCF}$	$\angle_{FCF}$
MCSCF	DZP	1.800	1.303	109.9	109.0
	DZP+*d*	1.793	1.304	110.0	109.0
	aug-DZP	1.812	1.307	109.9	109.0
	aug-DZP+*d*	1.807	1.308	109.9	109.0
	TZP	1.803	1.297	109.8	109.1
	TZP+*d*	1.800	1.297	109.9	109.1
	aug-TZP	1.815	1.298	109.8	109.1
	aug-TZP+*d*	1.812	1.298	109.8	109.1
MR-CISD	DZP	1.776	1.317	110.1	108.9
	DZP+*d*	1.768	1.317	110.1	108.8
	aug-DZP	1.778	1.323	110.2	108.7
	aug-DZP+*d*	1.770	1.324	110.3	108.6
	TZP	1.769	1.306	110.1	108.9
	TZP+*d*	1.766	1.306	110.1	108.8
	aug-TZP	1.774	1.307	110.1	108.8
	aug-TZP+*d*	1.771	1.307	110.1	108.8
MR-AQCC	DZP	1.774	1.330	110.2	108.8
	DZP+*d*	1.765	1.331	110.3	108.6
	aug-DZP	1.771	1.341	110.4	108.5
	aug-DZP+*d*	1.762	1.342	110.5	108.4
	TZP	1.767	1.321	110.2	108.6
	TZP+*d*	1.762	1.321	110.2	108.7
	aug-TZP	1.766	1.321	110.3	108.7
	aug-TZP+*d*	1.762	1.323	110.3	108.6
	Experimental[a]	1.751±0.005	1.328±0.002	110.3±0.4	108.6±0.4

[a]Reference 59.

empirically.[51–57] Once the couplings are obtained, the singlets' energies are corrected through second-order perturbation theory. According to this implementation, one has to input between which states the spin-orbit couplings are to be calculated. Consequently, such couplings only make sense for the CF_3Cl molecule, since for both CF_3 and chlorine fragments only the ground state is considered, and, besides, the kind of CF_3Cl excited states here considered (singlet and triplet $n\sigma^*$) is consequence of an interaction between the fragments. Therefore, in order to take the spin-orbit effect into account for the isolated fragments, we have used the approximation that only the chlorine atom is responsible for it. According to the tables given by Moore,[58] the ground state of the Cl atom is stabilized by 0.84 kcal/mol (0.0364 eV), as a consequence of spin-orbit coupling. Such assumption seems to be reasonable, since in the bonded CF_3Cl molecule the presence of spin-orbit effects is mainly due to the chlorine atom. Indeed, the stabilization energies due to the spin-orbit effect are 0.09 kcal/mol (0.0039 eV) and 0.38 kcal/mol (0.0165 eV) for the ground states of carbon and fluorine atoms, respectively.[58]

III. RESULTS AND DISCUSSION

A. Geometric parameters

The calculated ground state equilibrium geometrical parameters of CF_3Cl are given in Table I. Though C_s symmetry has been used in the calculations, the optimized structure has equal C–F distances, as well as equal $\angle_{FCF}$ and $\angle_{ClCF}$ bond angles (that is, a C_{3v} geometry has been obtained). As it can be seen from the results shown in this table, for a given basis set there is a tendency to a decrease in the C–Cl bond distance as more electron correlation is included (that is, in the order MCSCF→MR-CISD→MR-AQCC). An exception is found for the cc-pVDZ basis set, which is considered too small. An opposite trend has been obtained for the C–F bond distances. The inclusion of additional *d* functions in the standard cc-pVnZ and aug-cc-pVnZ sets has a small but non-negligible effect on the C–Cl bond distances, as expected. As can be seen from Table I, such inclusion leads to a decrease in the C–Cl bond distance. For the C–F bond distance such effect is much smaller and almost negligible, as expected, since the cc-pV(*n*+*d*)*Z* [and aug-cc-pV(*n*+*d*)*Z*] sets have been designed only for second row atoms.[40]

The effect of diffuse functions on the C–Cl bond distance is greater at the MCSCF level, probably due to the lack of dynamic electron correlation, and tends to increase the bond distance. At the MR-CISD level, the same trend holds, although to a lesser extension. On the other hand, at the MR-AQCC level, the diffuse functions lead to a shorter bond, and the effect is almost negligible if one compares the cc-pVTZ basis set with the aug-cc-pVTZ basis set. In the case of the C–F bonds, diffuse functions lead to an increase

in the bond lengths at all levels of theory considered. For the double-zeta basis set, the more accurate is the wave function, the greater is this effect (see Table I); for the triple-zeta basis set, the effect is essentially independent of the computational level. Very small changes have been observed for the bond angles, either varying the level of theory used or the basis set.

The global agreement between the optimized geometries and the experimental results is very good, the best performance being obtained at the MR-AQCC/aug-cc-pV$(T+d)Z$ level, which yielded C–Cl and C–F bond distances of 1.762 and 1.323 Å, respectively (those shall be compared with the experimental values of 1.751 and 1.328 Å, see Table I). The $\angle_{ClCF}$ and $\angle_{FCF}$ bond angles obtained with this method/basis set are 110.3° and 108.6°, also in excellent agreement with the corresponding experimental values [110.3° and 108.6° (Ref. 59)].

The present results can also be compared with those obtained by Roszak *et al.*[17] using the MP2 method along with relativistic effective core potentials (RECPs) that treats all but the ns^2np^5 shells in the core for F, Cl, and all but the $2s^22p^5$ shells in the core for the carbon atom.[60] Such RECP basis sets were supplemented by six-component *d* Gaussian functions adopted from Dunning and Hay[61] and by a set of diffuse *s* and *p* functions.[62] The best values obtained by Roszak *et al.*[17] were 1.748 Å, 1.342 Å, and 108.3° for C–Cl and C–F bond distances and $\angle_{FCF}$ bond angles, respectively. If one takes into account the standard deviations of the geometric parameters,[59] one can conclude that, concerning the C–Cl bond distance and the bond angles, the results of the present study are of similar quality to those of Roszak *et al.*[17] However, our calculations at the highest level [MR-AQCC/aug-cc-pV$(T+d)Z$] yield a far better description of the C–F bond distance [1.323 Å, compared to the experimental value of 1.328±0.002 Å, while the value obtained by Roszak *et al.* is 1.342 Å (Ref. 17)]. Roszak *et al.* also observed a small increase of 0.007 Å in the C–Cl bond distance when additional diffuse functions are included in the basis set and an almost negligible effect of such functions on both the C–F bond distances and $\angle_{FCF}$ bond angles. With the exception of the MR-AQCC calculations, the present results show a similar effect of the diffuse functions on the C–Cl bond distance.

In order to compute dissociation energies, enthalpies, and size-extensivity errors, full geometry optimizations have also been performed for the $CF_3\cdot$ radical, using the same computational methodologies and basis sets. Though the analysis of this geometry *per si* is not one of the aims of the present study, such analysis is important to assess the accuracy of the results in comparison with that of the CF_3Cl molecule, an important requisite in order to obtain consistent results concerning the three aforementioned quantities. As can be seen from Table II, the agreement between our best result (MR-AQCC/aug-cc-pVTZ, for which R_{CF}=1.313 Å and $\angle_{FCF}$=111.3°) and the experimental result [R_{CF}=1.318±0.002 Å, $\angle_{FCF}$=110.7±0.4° (Ref. 63)] is very good. There is also a good agreement between our MCSCF/cc-pVDZ results and the previous results obtained by Dixon[64] (see Table II) from restricted open-shell Hartree-Fock calculations using a double-zeta quality basis set augmented by a set of polarization functions.[61] Such agreement indicates the relatively small effect played by the static electron correlation on the geometry of the $CF_3\cdot$ radical.

TABLE II. Ground state equilibrium geometrical parameters of the $CF_3\cdot$ radical (distances in angstroms and angles in degrees). Abbreviations: DZP: cc-pVDZ, aug-DZP: aug-cc-pVDZ, TZP: cc-pVTZ, aug-TZP: aug-cc-pVTZ.

		R_{CF}	$\angle_{FCF}$
MCSCF	DZP	1.300	111.3
	aug-DZP	1.303	111.3
	TZP	1.291	111.5
	aug-TZP	1.290	111.5
MR-CISD	DZP	1.312	111.3
	aug-DZP	1.317	111.3
	TZP	1.298	111.6
	aug-TZP	1.299	111.4
MR-AQCC	DZP	1.325	111.1
	aug-DZP	1.333	111
	TZP	1.312	111.4
	aug-TZP	1.313	111.3
	Previous results[a]	1.300	111.4
	Experimental values[b]	1.318±0.002	110.7±0.4

[a]Reference 64.
[b]Reference 63.

B. Electronic parameters

1. Size-extensivity error

The values obtained for size-extensivity errors are shown in Table III. This error is defined as the energy difference between the optimized supermolecule and the isolated fragments ($CF_3\cdot$ and Cl·). It is worth to mention that the $CF_3\cdot$ fragment was found to have essentially the same geometry within the supermolecule and as an isolated species, which is a strong evidence for a negligible interaction between the $CF_3\cdot$ and Cl· fragments at the distance used in the supermolecule calculations (100 Å). As can be seen from Table III, size-extensivity corrections calculated at both the MR-CISD and MR-CISD+Q levels increase with the basis set size because of the larger percentage of electron correlation recovered.[65] At the MR-AQCC level, except for the aug-cc-pVTZ basis set the energy of the supermolecule is smaller than the sum of the fragments' energy (yielding a *negative*

TABLE III. Size-extensivity errors. Values in eV. Abbreviations: DZP: cc-pVDZ, aug-DZP: aug-cc-pVDZ, TZP: cc-pVTZ, aug-TZP: aug-cc-pVTZ.

	MR-CISD	MR-CISD+Q	MR-AQCC
DZP	0.924	0.405	−0.0174
DZP+*d*	0.974	0.437	−0.0153
aug-DZP	1.097	0.537	−0.0161
aug-DZP+*d*	1.156	0.579	−0.0135
TZP	1.474	0.759	−0.0124
TZP+*d*	1.497	0.782	−0.0115
aug-TZP	1.531	0.810	0.0193
aug-TZP+*d*	1.553	0.831	−0.0119

TABLE IV. Calculated values of vertical excitation energy ($\Delta E_{\text{vertical}}$), dissociation energy ($\Delta E_{\text{diss}}$), dissociation enthalpy (ΔH_{diss}), including zero-point energies, and oscillator strength (f). Values in eV. Abbreviations: DZP: cc-pVDZ, aug-DZP: aug-cc-pVDZ, TZP: cc-pVTZ, aug-TZP: aug-cc-pVTZ, DZP+d: cc-pV(D+d)Z, aug-DZP+d: aug-cc-pV(D+d)Z, TZP+d: cc-pV(T+d)Z, aug-TZP+d: aug-cc-pV(T+d)Z. Scaling factors for vibrational frequencies: CASSCF/DZP, CASSCF/DZP+d, CASSCF/TZP, and CASSCF/TZP+d 0.889; CASSCF/aug-DZP, CASSCF/aug-DZP+d, CASSCF/aug-TZP, and CASSCF/aug-TZP+d 0.882; MR-CISD/DZP, MR-CISD/DZP+d, MR-CISD/TZP, and MR-CISD/TZP+d 0.918; MR-CISD/aug-DZP, MR-CISD/aug-DZP+d, MR-CISD/aug-TZP, and MR-CISD/aug-TZP+d 0.916; MR-AQCC/DZP, MR-AQCC/DZP+d, MR-AQCC/TZP, and MR-AQCC/TZP+d 0.960; MR-AQCC/aug-DZP, MR-AQCC/aug-DZP+d, MR-AQCC/aug-TZP, and MR-AQCC/aug-TZP+d 0.968. Values in parenthesis include spin-orbit+BSSE corrections. Spin-orbit correction obtained from CASSCF calculations has been used for the other methods.

		MCSCF	MR-CISD	MR-CISD+Q	MR-AQCC
$\Delta E_{\text{vertical}}$	DZP	7.91	8.24	8.24	8.19
	DZP+d	7.96	8.26	8.24	8.19
	aug-DZP	7.50	7.81	7.78	7.64
	aug-DZP+d	7.50	7.79	7.74	7.67
	TZP	7.78	8.08	8.03	7.95
	TZP+d	7.77	8.05	7.99	7.91
	aug-TZP	7.50	7.82	7.76	7.67
	aug-TZP+d	7.48	7.78	7.71	7.63
	Experimental[a]		7.7±0.1		
ΔE_{diss}	DZP	2.64 (2.53)	3.18 (2.95)	3.33 (3.08)	3.37 (3.18)
	DZP+d	2.69 (2.58)	3.23 (2.98)	3.38 (3.11)	3.41 (3.14)
	aug-DZP	2.65 (2.55)	3.27 (3.10)	3.43 (3.25)	3.47 (3.29)
	aug-DZP+d	2.69 (2.59)	3.32 (3.11)	3.48 (3.27)	3.51 (3.30)
	TZP	2.76 (2.70)	3.37 (3.25)	3.54 (3.41)	3.57 (3.44)
	TZP+d	2.78 (2.72)	3.40 (3.29)	3.56 (3.44)	3.60 (3.48)
	aug-TZP	2.73 (2.68)	3.41 (3.34)	3.59 (3.52)	3.66 (3.52)
	aug-TZP+d	2.75 (2.70)	3.44 (3.37)	3.61 (3.54)	3.65 (3.53)
ΔH_{diss}	DZP	2.71 (2.60)	3.25 (3.02)	3.40 (3.15)	3.43 (3.24)
	DZP+d	2.75 (2.64)	3.30 (3.05)	3.44 (3.18)	3.48 (3.21)
	aug-DZP	2.72 (2.62)	3.34 (3.17)	3.50 (3.32)	3.54 (3.36)
	aug-DZP+d	2.76 (2.66)	3.38 (3.18)	3.54 (3.33)	3.58 (3.37)
	TZP	2.82 (2.76)	3.44 (3.32)	3.60 (3.47)	3.64 (3.51)
	TZP+d	2.85 (2.78)	3.47 (3.36)	3.63 (3.51)	3.66 (3.54)
	aug-TZP	2.79 (2.74)	3.48 (3.41)	3.65 (3.58)	3.72 (3.59)
	aug-TZP+d	2.81 (2.76)	3.50 (3.43)	3.68 (3.61)	3.72 (3.59)
	Experimental[b]		3.68		
f	DZP	7.13×10^{-3}	6.17×10^{-4}	⋯	⋯
	aug-DZP	1.56×10^{-2}	3.83×10^{-3}	⋯	⋯
	TZP	1.33×10^{-2}	2.74×10^{-3}	⋯	⋯
	Experimental[a]		$3.12\times10^{-3}\pm2.50\times10^{-4}$		

[a]Reference 12.
[b]Reference 72.

size-extensivity error), and such difference decreases (in absolute value) in the order cc-pVDZ > aug-cc-pVDZ > cc-pVTZ (see Table III). The same trend holds for the newly developed basis sets, that is, the cc-pV(n+d)Z, along with their augmented counterparts. The aug-cc-pVTZ basis set yields results that are *qualitatively* different from the previous ones, in the sense that in this case the energy of the supermolecule is greater than that of the isolated fragments. It can thus be expected that more flexible basis sets (i.e., cc-pVQZ and aug-cc-pVQZ) would again decrease these *positive* size-extensivity errors. The most important result at this point is that the MR-AQCC size-extensivity errors are *much smaller* than the corresponding errors resulting from the MR-CISD+Q approach, a result that has been also found, for example, in the study of the Cope rearrangement of 1,5-hexadiene.[66]

2. Vertical excitation energy, dissociation energy, dissociation enthalpy, and oscillator strength

Calculated values of vertical excitation energies ($\Delta E_{\text{vertical}}$), dissociation energies (ΔE_{diss}), dissociation enthalpies (ΔH_{diss}), and oscillator strengths (f) are collected in Table IV. The values of $\Delta E_{\text{vertical}}$, ΔE_{diss}, and ΔH_{diss} include

TABLE V. BSSE and spin-orbit (SO) corrections. Values in eV. Abbreviations: DZP: cc-pVDZ, aug-DZP: aug-cc-pVDZ, TZP: cc-pVTZ, aug-TZP: aug-cc-pVTZ, DZP+*d*: cc-pV(*D*+*d*)*Z*, aug-DZP+*d*: aug-cc-pV(*D*+*d*)*Z*, TZP+*d*: cc-pV(*T*+*d*)*Z*, aug-TZP+*d*: aug-cc-pV(*T*+*d*)*Z*.

	MCSCF				MR-CISD+Q	
	BSSE	SO_{vert}	SO_{diss}	MR-CISD	BSSE	MR-AQCC
DZP	−0.0737	0.001 668	−0.036 04	−0.1951	−0.2126	−0.1565
DZP+*d*	−0.0746	0.001 570	−0.036 04	−0.2119	−0.2324	−0.2308
aug-DZP	−0.0606	0.001 690	−0.036 02	−0.1360	−0.1416	−0.1417
aug-DZP+*d*	−0.0610	0.001 598	−0.036 03	−0.1698	−0.1778	−0.1771
TZP	−0.0275	0.001 556	−0.036 03	−0.0879	−0.0977	−0.0980
TZP+*d*	−0.0277	0.001 508	−0.036 04	−0.0751	−0.0842	−0.0851
aug-TZP	−0.0176	0.001 558	−0.036 04	−0.0354	−0.0382	−0.1041
aug-TZP+*d*	−0.0177	0.001 510	−0.036 05	−0.0355	−0.0384	−0.0886

zero-point energies. Spin-orbit coupling and BSSE corrected values are also shown in this table. The vibrational frequencies obtained with the cc-pVTZ basis set have been used in the zero-point and termochemical calculations with the aug-cc-pVTZ basis set. Concerning the vibrational frequencies, scale factors obtained for CASSCF, MR-CISD, and MR-AQCC methods along with the cc-pVDZ and aug-cc-pVDZ basis sets have been determined such that the zero-point energies of CF_3Cl computed with the PBE0/cc-pVDZ and PBE0/aug-cc-pVDZ methods and scaled with the recommended factors of 0.962 and 0.961 (Ref. 67) were reproduced. The PBE0 functional[68] has been chosen on the basis of the smallest root mean square error.[67] The obtained scale factors are listed in the footnote of Table IV and have also been used for the $CF_3\cdot$ radical and for the corresponding triple-zeta and *d*-extended basis sets (since it has been found that they do not depend significantly on the basis set considered[67]), in order to compute zero-point energies and dissociation enthalpies (ΔH_{diss}). The equations used for computing thermochemical data assume noninteracting particles (ideal gas) and are covered in detail in the book by McQuarrie and Simon.[69]

3. BSSE results

As aforementioned, the CP correction has been applied only in order to obtain BSSE corrected dissociation energies (and enthalpies). The corresponding values are listed in Table V. These corrections lower the computed dissociation energies (and enthalpies) and all discussions here presented refer to their absolute values. As expected, the general trend is a decrease of the CP correction as the basis set size increases. The exception is found for the MR-AQCC results with triple-zeta basis sets. In these cases, the BSSE values increase very slightly as additional diffuse functions are included in the cc-pVTZ and cc-pV(*T*+*d*)*Z* basis sets (by 0.0061 eV and 0.0035 eV, respectively; see Table V). The basis set superposition error range from 0.0177 eV [MCSCF/aug-cc-pV(*T*+*d*)*Z*] to 0.2324 eV [MR-CISD+*Q*/cc-pV(*D*+*d*)*Z*], and the smaller values are obtained with the MCSCF method. The inclusion of additional *d* functions in the cc-pVDZ and aug-cc-pVDZ basis sets increases the BSSE values, at all computational levels. For the cc-pVTZ basis set such effect is practically negligible at the MCSCF level, and for the other methods there is a decrease of at most 0.0135 eV (at MR-CISD+Q level). For the aug-cc-pVTZ basis sets such effect is almost negligible and not greater than 0.0002 eV, for all but the MR-AQCC method. For this latter method there is a decrease of 0.0155 eV. Therefore, the inclusion of additional *d* functions in the standard correlation consistent basis sets seems to be important in obtaining highly accurate dissociation energies of molecules including second row atoms.

It is clear from the results shown in Table IV that the additional diffuse functions present in the augmented versions of the studied basis sets play an important role in the description of the $n\sigma^*$ state, leading to a decrease in the value of $\Delta E_{vertical}$, which ranges from 0.26 eV (MR-CISD/cc-pVTZ→MR-CISD/aug-cc-pVTZ) to 0.47 eV [MR-AQCC/cc-pV(*D*+*d*)*Z*→MR-AQCC/aug-cc-pV(*D*+*d*)*Z*]. The results at the MR-CISD level are 0.28–0.33 eV greater than the corresponding MCSCF results, indicating, as expected, a significant and almost constant effect of the dynamic electronic correlation in $\Delta E_{vertical}$. The importance of such effect also becomes evident if one looks at the dependence of the MCSCF results on the size of the used basis set. Similarly to what is obtained for the other methods, in this case, the inclusion of additional diffuse functions is more important than the extension of the basis set from double- to triple-zeta quality. However, in the case of the MCSCF method, the increase of the basis set by including additional diffuse functions leads to a poorer agreement with the experimental result. Except for the cc-pVDZ basis set, the inclusion of additional *d* functions decreases the values of $\Delta E_{vertical}$, even though the effect is very small and not greater than 0.05 eV (see Table IV). Size-extensivity corrections are also important and tend to decrease the obtained values of $\Delta E_{vertical}$. The decrease due to the extended Davidson correction (MR-CISD+Q) is small but becomes more pronounced for larger basis sets, ranging from zero to 0.07 eV (see Table V). The MR-AQCC results show a further decrease in the calculated $\Delta E_{vertical}$ values, with the largest decrease obtained with the aug-cc-pVDZ basis set (0.14 eV), followed by the triple-zeta basis sets (0.09 eV for aug-cc-pVTZ and 0.08 eV for the remaining ones). The highest level result obtained in this study [7.63 eV; MR-AQCC/aug-cc-pV(*T*+*d*)*Z*] is in very good

agreement with the experimental value of 7.7±0.1 eV.[12] The most accurate result obtained in this study for the oscillator strength ($f=2.74\times10^{-3}$) was obtained at the MR-CISD/cc-pVTZ level, being also in very good agreement with the experimental value of $3.12\times10^{-3}\pm2.50\times10^{-4}$.[12] Spin-orbit corrections for $\Delta E_{\text{vertical}}$ are smaller than 1.67×10^{-3} eV (see Table V), and thus negligible. One of the reasons for such a small correction is the large energy differences between singlet and triplet states in the ground state equilibrium geometry [for instance, $E(1\,^3A')$-$E(1\,^1A')=6.94$ eV and $E(2\,^1A')$-$E(1\,^3A')=1.02$ eV, at CASSCF/aug-cc-pV$(T+d)Z$ level], since the calculated spin-orbit matrix elements are smaller than 300 cm^{-1} (0.037 eV).

Both basis set size and size-extensivity corrections tend to increase the calculated values of ΔE_{diss} and ΔH_{diss}, at all levels of theory employed (see Table IV). The most accurate value (neglecting spin-orbit and BSSE corrections) now obtained for ΔE_{diss} [3.65 eV, at MR-AQCC/aug-ccpV$(T+d)Z$ level] is somewhat lower than the corresponding value of 4.014 eV obtained by Roszak *et al.*[17] at MP2/aug-cc-pVTZ level. Spin-orbit corrections decrease the calculated values of ΔE_{diss} by about 3.6×10^{-2} eV (0.83 kcal/mol), and such correction is practically independent of the computational level and the basis set used (see Table V). Such value is consistent with the total spin-orbit correction of about 0.9 kcal/mol for the dissociation energy (and enthalpy) of the CCl molecule reported by Dixon and Peterson,[70] obtained from scalar relativistic corrections [from CISD(FC)/unc-aug-cc-pV$(Q+d)Z$ calculations] and correction due to the incorrect treatment of the atomic asymptotes as an average of spin multiplets. Similar calculations performed by Feller *et al.*[71] obtained total spin-orbit corrections of at most 1.4 kcal/mol for small halogenated molecules containing one chlorine atom and lighter elements. Even though our estimates of the spin-orbit correction are of lower quality than the ones reported by Dixon and Peterson[70] and Feller *et al.*[71] it is not expected, based on the results presented by these authors, a correction greater than twice the one here presented (that is, of about 7.0×10^{-2} eV). Since ΔE and ΔH are interconnected, and since our best estimated value for ΔH_{diss} [3.59 eV, MR-AQCC/aug-cc-pV$(T+d)Z$+spin-orbit and BSSE corrections] is in very good agreement with the experimental value of 3.68 eV,[72] it is thus expected that the value now obtained for ΔE_{diss} (3.65 eV), without spin-orbit and BSSE corrections, is, in fact, more accurate than the corresponding value obtained by Roszak *et al.* (4.014 eV).[17]

C. Potentials energy curves

Figure 1 shows the potential energy curves along the C–Cl bond distance, for the S_0 and S_1 states ($1\,^1A_1$ and $1\,^1E$, in C_{3v} symmetry) at the MR-AQCC level of approximation with the cc-pVTZ and cc-pV$(T+d)Z$ basis sets. The potential energy profiles obtained with the other methods and basis sets are very similar and thus are not shown. As mentioned before, only C_s symmetry has been imposed at all computational levels (with the corresponding $1\,^1A'$, $2\,^1A'$, and $1\,^1A''$ notations for the states). Upon either full geometry optimization (ground state) or relaxed potential energy calculations,

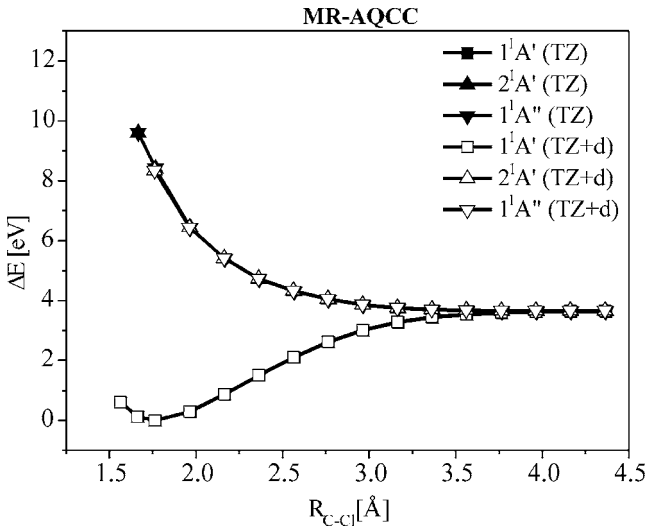

FIG. 1. Potential energy profiles of S_0 and S_1 states calculated at MR-AQCC/cc-pVTZ and MR-AQCC/cc-pV$(T+d)Z$ levels as a function of C–Cl distance, under C_s symmetry restriction. The energies are refereed to the energies obtained at the ground state equilibrium geometry of each basis set. In this plot the values obtained with these two basis sets are practically coincident. Notice that the $2\,^1A'$ and the $1\,^1A''$ states remain degenerate, since the C_{3v} symmetry is not broken.

the C_{3v} symmetry was not broken, so the $2\,^1A'$ and $1\,^1A''$ states remained degenerate. The Jahn-Teller effect[73] is observed when one tries to optimize the geometries of $2\,^1A'$ or $1\,^1A''$ state: the state which is being optimized has its energy lowered (as compared with the energy at the ground state geometry), while the energy of the other state energy is raised, as a consequence of symmetry lowering from C_{3v} to C_s (the symmetry plane contains one atom of each type). If the C–Cl distance is fixed during the optimization procedure, a local minimum is obtained, as expected. However, when all degrees of freedom are relaxed, the optimization procedure leads to a continuous increase of the C–Cl distance, with a corresponding energy lowering, thus characterizing a dissociative state.

Figure 2 shows the crossing region of the potential energy curves of S_0 and S_1 states, obtained at all four computational levels here employed. The results obtained with the aug-cc-pVTZ basis set are from single-point calculations performed at the geometry generated with the cc-pVTZ basis set. The same holds for the aug-cc-pV$(T+d)Z$ basis set. It is evident that the crossing, as well as the S_1 state well depth, seems to vanish as the basis set size increases, for both cc-pVnZ and cc-pV$(n+d)Z$ series. The series of results obtained with the cc-pVnZ and cc-pV$(n+d)Z$ basis sets are very similar, as they are in the case of the augmented basis set versions. If the energy differences between S_0 and S_1, after the crossing point, are compared, one can clearly see that they decrease as more electronic correlation is included in the wave function (see Fig. 2). The results obtained at MR-AQCC/aug-cc-pV$(T+d)Z$ and MR-AQCC/aug-cc-pVTZ levels are the most accurate ones and practically show no crossing along the C–Cl coordinate. It can then be expected that upon extrapolation of the results to the complete basis set limit, for instance, with a two-point fit based on the cc-pVTZ and cc-pVQZ results [the so-called (TQ)

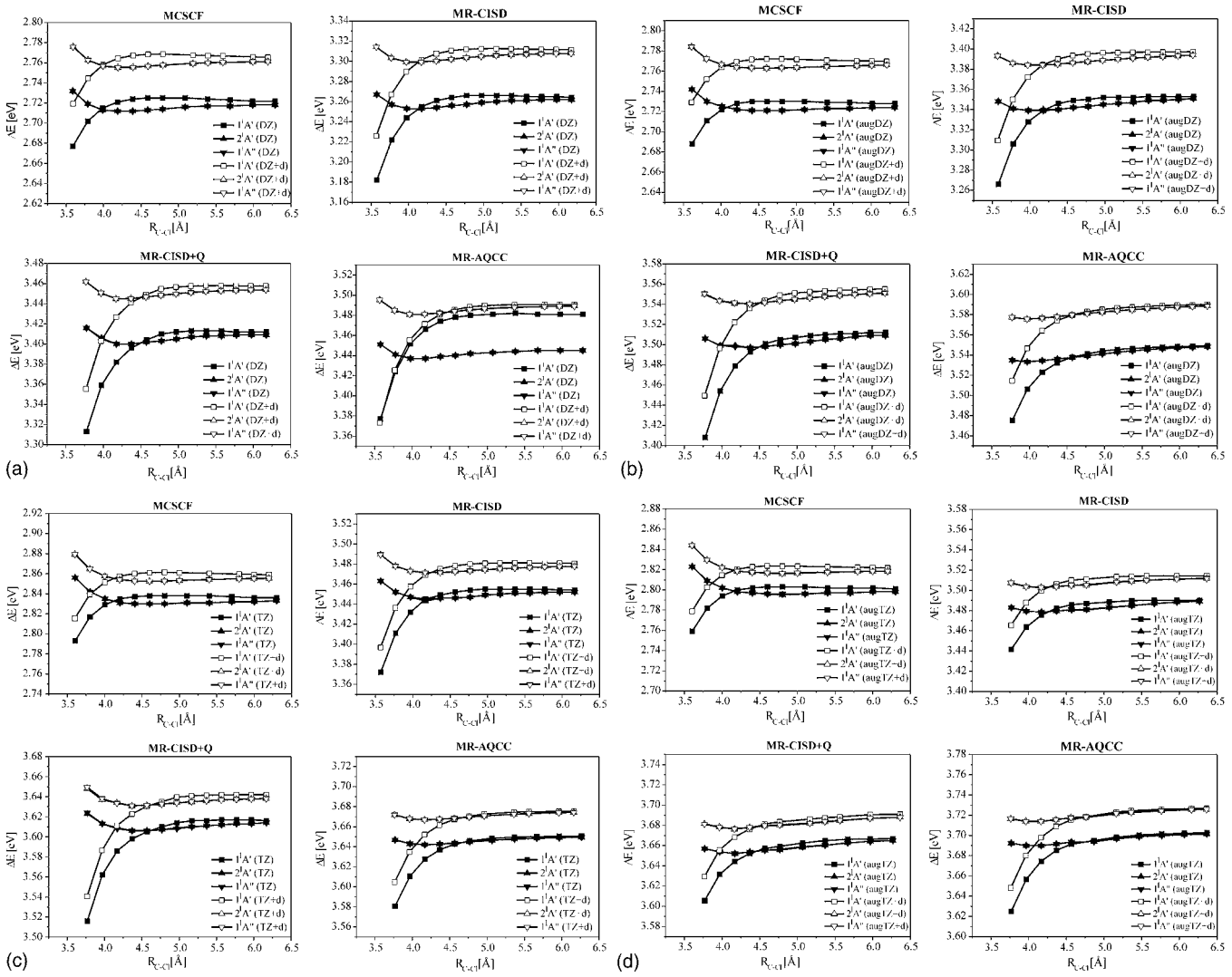

FIG. 2. Potential energy profiles in the region around the crossing point of S_0 and S_1 states as a function of C–Cl distance, under C_s symmetry restriction. Notice that the $2\,^1A'$ and the $1\,^1A''$ states remain degenerate, since the C_{3v} symmetry is not broken.

extrapolation[74–77]], no S_0/S_1 crossing and no S_1 well depth should occur, along the C–Cl coordinate only. In the case of MR-AQCC calculations, such extrapolation is likely to be required only to vanish the very small S_1 well depth that still remains with the largest basis sets (see Fig. 2). Unfortunately, such extrapolation technique requires results obtained with the aug-cc-pVQZ basis set, whose calculations were not affordable due to the size of the system. Spin-orbit effects are expected to cause a further split between $^1A_1$ and ^1E $(n\sigma^*)$ states upon dissociation.[33] Besides, a singlet to triplet conversion upon dissociation is also possible, yielding Cl atoms in the $^2P_{1/2}$ state, in contrast with the $^2P_{3/2}$ state resulting from the dissociation of the ground and ^1E singlet states.[33] However, based on the magnitude of the spin-orbit coupling matrix elements obtained in this study (lower than 300 cm^{-1}) such conversion should have a very small probability.

Crossings between electronic states of polyatomic molecules are multidimensional problems and cannot be fully analyzed using one coordinate only (in this case the C–Cl distance). In order to deal with this problem more properly, we have searched for a conical intersection geometry (at several intermediate geometry regions, starting either with a C_{3v} geometry or with a C_s geometry) using gradient driven techniques, at MCSCF and MR-CISD levels, as described in Refs. 78 and 79. C_s and C_1 symmetries have been used in these calculations, for both geometries (C_s and C_{3v}). The geometry optimization steps show a continuous increase in the C–Cl distance, with a corresponding energy difference decrease and an oscillatory behavior of both energies (of ground and first excited state). These features, along with the nonconvergence of the optimization at the crossing seam procedure, seem to indicate an absence of crossing between ground and $n\sigma^*$ states in the intermediate geometry regions, at the two symmetries employed (C_s with the symmetry plane containing one atom of each type as well as without symmetry, C_1). This result does not exclude the occurrence of crossings at other regions of the potential energy surface, but it is an important evidence in favor of its absence. This problem will be covered in more detail in a further and extended investigation concerning the three states considered in our calculations.

IV. CONCLUSIONS

Highly accurate multireference (MR-CISD, MR-CISD+Q, and MR-AQCC) and multiconfigurational (CASSCF) calculations have been applied to the study of ground state equilibrium geometry and dissociation of the ground and first excited ($n\sigma^*$) singlet states of the CF_3Cl molecule. Spin-orbit, BSSE, and extensivity corrections have been considered. The ground state geometry of CF_3Cl was, for the first time, fully optimized at CASSCF, MR-CISD, and MR-AQCC levels. The results now obtained concerning the C–Cl bond distance and the $\angle_{FCF}$ bond angles (1.762 Å and 108.6°, respectively, at the MR-AQCC/aug-cc-pVTZ level) are of similar quality to those of Roszak *et al.*[17] (the best values obtained by these authors were 1.748 Å and 108.3°). However, the highest level [MR-AQCC/aug-cc-pV$(T+d)Z$] calculations now reported yield a far better description of the C–F bond distance [1.323 Å compared to the experimental value of 1.328±0.002 Å (Ref. 59)] when compared with the value obtained by Roszak *et al.* [1.342 Å (Ref. 17)]. The basis set effects on the geometric parameters have also been considered in the present study and were found to be more important for the bond distances than for the bond angles.

The calculated size-extensivity errors upon dissociation showed the importance of performing a very accurate size-extensivity correction, as is included in the MR-AQCC approach, and also demonstrated the superiority of this method, as compared to the MR-CISD+Q method.

Vertical excitation energies ($\Delta E_{vertical}$), dissociation energies (ΔE_{diss}), dissociation enthalpies (ΔH_{diss}), and oscillator strengths (f) were also calculated and compared with the available experimental (for $\Delta E_{vertical}$, ΔH_{diss}, and f) and theoretical (for ΔE_{diss}) results. The best results now obtained for $\Delta E_{vertical}$ [7.63 eV, at the MR-AQCC/aug-cc-pV$(T+d)Z$ level], ΔH_{diss} (3.59 eV, MR-AQCC/aug-cc-pVTZ), and f (2.74×10^{-3}, MR-CISD/cc-pVTZ) are in very good agreement with the corresponding experimental results (7.7±0.1 eV,[12] 3.68 eV,[72] and $3.12\times10^{-3}\pm2.50\times10^{-4}$).[12] Our most accurate value for ΔE_{diss} [3.65 eV, MR-AQCC/aug-ccpV$(T+d)Z$], neglecting spin-orbit and BSSE corrections, is somewhat lower than the corresponding value of 4.014 eV obtained by Roszak *et al.*[17] at the MP2/aug-cc-pVTZ level. Since ΔE and ΔH are interconnected, it can be expected a greater accuracy in the calculation of ΔE_{diss} at the highest computational level now employed. Size-extensivity effects were found to be important for $\Delta E_{vertical}$, ΔE_{diss}, and ΔH_{diss}. They tend to decrease $\Delta E_{vertical}$ and increase ΔE_{diss} and ΔH_{diss}. Inclusion of additional diffuse functions in the augmented versions of the basis sets used in the present study gives rise to similar effects on these properties. Spin-orbit corrections have a practically negligible effect on $\Delta E_{vertical}$ and lower the dissociation enthalpies and energies by an almost constant value of about 3.6×10^{-2} eV (0.83 kcal/mol). BSSE correction represents a further and larger decrease on these energies of at most 0.2324 eV [MR-CISD+Q/cc-pV$(D+d)Z$]; the smaller corrections were obtained at the CASSCF level.

The relaxed potential energy curves (along the C–Cl bond) for the first two singlet states have been also computed. The crossing between the S_0 and S_1 states, along with the well depth of S_1, is qualitatively influenced by the basis set size at all computational levels investigated. The present results clearly show a tendency toward an absence of crossing and toward a fully dissociative pattern for S_1 (along the C–Cl coordinate only), as the basis set size increases. The inclusion of dynamic electronic correlation (especially at MR-AQCC level) is also important in obtaining no crossing in the intermediate region, along the C–Cl coordinate. Spin-orbit effects should lead to a further split between S_0 and S_1 states.[33] An additional and more realistic investigation of a possible crossing between S_0 and S_1 states has been also performed using a gradient driven technique, at MCSCF and MR-CISD levels,[78,79] and the results point also toward an absence of crossing in the intermediate C–Cl region.

ACKNOWLEDGMENTS

One of the authors (E.V.) would like to thank a fellowship provided by the FAPESQ/CNPq (Brazilian agency) within the framework of the DCR program. The authors acknowledge support by CAPES/GRICES. They are also grateful to Dr. Thomas Mueller (Central Institute for Applied Mathematics-Research Center, Juelich) for his valuable suggestions concerning the calculations. R.F. acknowledges financial support from FCT (Research Project No. POCI/QUI/58937/2004) and FEDER.

[1] M. J. Molina and F. S. Rowland, Nature (London) **249**, 810 (1974).
[2] F. S. Rowland, Annu. Rev. Phys. Chem. **42**, 731 (1991).
[3] L. T. Molina and M. J. Molina, J. Phys. Chem. **91**, 433 (1987).
[4] J. C. Farman, B. G. Gardiner, and J. D. Shanklin, Nature (London) **315**, 207 (1985).
[5] J. Mitchell, T. Johns, J. Gregory, and S. Tett, Nature (London) **376**, 501 (1995).
[6] S. Tett, P. Stott, M. Allen, W. Ingram, and J. Mitchell, Nature (London) **399**, 569 (1999).
[7] L. T. Molina and M. J. Molina, J. Geophys. Res. **91**, 14501 (1986).
[8] J. Doucet, P. Sauvageau, and C. Sandorfy, J. Chem. Phys. **58**, 3708 (1973).
[9] R. Gilbert, P. Sauvageau, and C. Sandorfy, J. Chem. Phys. **60**, 4820 (1974).
[10] T. Ibuki, A. Hiraya, and K. Shobatake, J. Chem. Phys. **90**, 6290 (1989).
[11] J. F. Ying and K. T. Leung, J. Chem. Phys. **101**, 8333 (1994).
[12] J. F. Ying, C. P. Mathers, K. T. Leung, H. P. Pritchard, C. Winstead, and V. McKoy, Chem. Phys. Lett. **212**, 289 (1993).
[13] J. F. Ying and K. T. Leung, J. Chem. Phys. **100**, 7120 (1994).
[14] J. F. Ying and K. T. Leung, J. Chem. Phys. **100**, 1011 (1994).
[15] M. Suto and L. C. Lee, J. Chem. Phys. **79**, 1127 (1983).
[16] M. Suto, N. Washida, H. Akimoto, and M. Nakamura, J. Chem. Phys. **78**, 1019 (1983).
[17] S. Roszak, W. S. Koski, J. J. Kaufman, and K. Balasubramanian, J. Chem. Phys. **106**, 7709 (1997).
[18] S. S. Kumaran, M.-C. Su, K. P. Lim, J. V. Michael, A. F. Wagner, L. B. Harding, and D. A. Dixon, J. Phys. Chem. **100**, 7541 (1996).
[19] M. W. Schmidt and M. S. Gordon, Annu. Rev. Phys. Chem. **49**, 233 (1998).
[20] I. Shavitt, in *Methods of Electronic Structure Theory*, edited by H. F. Schaefer III (Plenum, New York, 1976), p. 189.
[21] S. R. Langhoff and E. R. Davidson, Int. J. Quantum Chem. **8**, 61 (1974).
[22] P. J. Bruna, S. D. Peyerimhoff, and R. J. Buenker, Chem. Phys. Lett. **72**, 278 (1981).
[23] P. G. Szalay and R. J. Bartlett, Chem. Phys. Lett. **214**, 481 (1993).
[24] P. G. Szalay and R. J. Bartlett, J. Chem. Phys. **103**, 3600 (1995).
[25] P. G. Szalay, T. Mueller, and H. Lischka, Phys. Chem. Chem. Phys. **2**, 2067 (2000).
[26] L. Fusti-Molnar and P. G. Szalay, J. Phys. Chem. **100**, 6288 (1996).
[27] L. Fusti-Molnar and P. G. Szalay, Chem. Phys. Lett. **258**, 400 (1996).

[28] R. Shepard, H. Lischka, P. G. Szalay, T. Kovar, and M. Ernzerhof, J. Chem. Phys. **96**, 2085 (1992).
[29] R. Shepard, in *Modern Electronic Structure Theory*, edited by D. R. Yarkony, (World Scientific, Singapore, 1995), pt. 1, p. 345.
[30] M.-W. Yen, P. M. Johnson, and M. G. White, J. Chem. Phys. **99**, 126 (1993).
[31] Y. Matsumi, K. Tonokura, and M. Kawasaki, J. Chem. Phys. **94**, 2669 (1991).
[32] P. Brewer, P. Das, G. Ondrey, and R. Bersohn, J. Chem. Phys. **79**, 720 (1983).
[33] Y. Amatatsu, K. Morokuma, and S. Yabushita, J. Chem. Phys. **94**, 4858 (1990).
[34] H. Lischka, A. J. A. Aquino, M. Barbatti, and M. Solimannejad, Lect. Notes Comput. Sci. **3480**, 1004 (2005).
[35] M. Barbatti, J. Paier, and H. Lischka, J. Chem. Phys. **121**, 11614 (2004).
[36] A. M. Velasco, E. Mayor, and I. Martin, Chem. Phys. Lett. **377**, 189 (2003).
[37] H. Lischka, M. Dallos, and R. Shepard, Mol. Phys. **100**, 1647 (2002).
[38] T. H. Dunning, Jr., J. Chem. Phys. **90**, 1007 (1989).
[39] R. A. Kendall, T. H. Dunning, Jr., and R. J. Harrison, J. Chem. Phys. **96**, 6796 (1992).
[40] T. H. Dunning, K. A. Peterson, Jr., and A. K. Wilson, J. Chem. Phys. **114**, 9244 (2001).
[41] H. Lischka, R. Shepard, F. B. Brown, and I. Shavitt, Int. J. Quantum Chem., Quantum Chem. Symp. **15**, 91 (1981).
[42] R. Shepard, I. Shavitt, R. M. Pitzer, D. C. Comeau, M. Pepper, H. Lischka, P. G. Szalay, R. Alrichs, F. B. Brown, and J. Zhao, Int. J. Quantum Chem., Quantum Chem. Symp. **22**, 149 (1988).
[43] H. Lischka, R. Shepard, I. Shavitt *et al.*, COLUMBUS, an *ab initio* electronic structure program, Release 5.9, 2003.
[44] H. Lischka, R. Shepard, R. M. Pitzer, I. Shavitt, M. Dallos, T. Müller, Péter G. Szalay, M. Seth, G. S. Kedziora, S. Yabushita, and Z. Zhang-Phys. Chem. Chem. Phys. **3**, 664 (2001).
[45] T. Helgaker, H. J. Aa Jensen, P. Jørgensen, J. Olsen, K. Ruud, H. Agren, T. Andersen, K. L. Bak, V. Bakken, O. Christiansen, P. Dahle, E. K. Dalskov, T. Enevoldsen, B. Fernandez, H. Heiberg, H. Hettema, D. Jonsson, S. Kirpekar, R. Kobayashi, H. Koch, K. V. Mikkelsen, P. Norman, M. J. Packer, T. Saue, P. R. Taylor, and O. Vahtras, DALTON, an *ab initio* electronic structure program, Release 1.0, 1997.
[46] G. Fogarasi, X. Zhou, P. W. Taylor, and P. Pulay, J. Am. Chem. Soc. **114**, 8191 (1992).
[47] P. Császár and P. Pulay, J. Mol. Struct. **114**, 31 (1984).
[48] H. B. Jansen and P. Ross, Chem. Phys. Lett. **3**, 140 (1969).
[49] S. B. Boys and F. Bernardi, Mol. Phys. **19**, 553 (1970).
[50] P. Salvador, B. Paizs, M. Duran, and S. Suhai, J. Comput. Chem. **22**, 765 (2001).
[51] P. W. Abegg, Mol. Phys. **30**, 579 (1975).
[52] T. E. Walker and W. G. Richards, J. Chem. Phys. **52**, 1311 (1970).
[53] P. W. Abegg and T.-K. Ha, Mol. Phys. **27**, 763 (1974).
[54] R. Cimiraglia, M. Persico, and J. Tomasi, Chem. Phys. Lett. **76**, 169 (1980).
[55] S. Koseki, M. W. Schmidt, and M. S. Gordon, J. Phys. Chem. **96**, 10768 (1992).
[56] S. Koseki, M. S. Gordon, M. W. Schmidt, and N. Matsunaga, J. Phys. Chem. **99**, 12764 (1995).
[57] S. Koseki, M. W. Schmidt, and M. S. Gordon, J. Phys. Chem. **102**, 10430 (1998).
[58] C. E. Moore, *Atomic Energy Levels* (National Bureau of Standards, Washington, DC, 1971).
[59] L. S. Bartell and L. O. Brockway, J. Chem. Phys. **23**, 1860 (1955).
[60] L. F. Pacios and P. A. Christiansen, J. Chem. Phys. **82**, 2664 (1985).
[61] T. H. Dunning, Jr. and P. J. Hay, in *Methods of Electronic Structure Theory*, edited by H. F. Schaefer III (Plenum, New York, 1977), p. 1.
[62] M. J. Frisch, J. A. Pople, and J. S. Binkley, J. Chem. Phys. **80**, 3265 (1984).
[63] C. Yamada and E. Hirota, J. Chem. Phys. **78**, 1703 (1983).
[64] D. A. Dixon, J. Chem. Phys. **83**, 6055 (1985).
[65] T. Mueller, M. Dallos, and H. Lischka, J. Chem. Phys. **110**, 7176 (1999).
[66] E. Ventura, S. A. do Monte, M. Dallos, and H. Lischka, J. Phys. Chem. A **107**, 1175 (2003).
[67] Y. Tantirungrotechai, K. Phanasant, S. Roddecha, P. Surawatanawong, V. Sutthikhum, and J. Limtrakul, J. Mol. Struct.: THEOCHEM **760**, 189 (2006).
[68] J. P. Perdew, K. Burke, and M. Ernzerhof, Phys. Rev. Lett. **77**, 3865 (1996); **78**, 1396 (1997).
[69] D. A. McQuarrie and J. D. Simon, *Molecular Thermodynamics* (University Science Books, New York, NY, 1999).
[70] D. A. Dixon and K. A. Peterson, J. Chem. Phys. **115**, 6327 (2001).
[71] D. Feller, K. A. Peterson, W. A. de Long, and D. A. Dixon, J. Chem. Phys. **118**, 3510 (2003).
[72] H. Okabe, *Photochemistry of Small Molecules* (Wiley, New York, 1978), pp. 375–380.
[73] H. A. Jahn and E. Teller, Proc. R. Soc. London, Ser. A **161**, 220 (1937).
[74] A. Halkier, T. Helgaker, P. Jørgensen, W. Klopper, H. Koch, and J. Olsen, Chem. Phys. Lett. **286**, 243 (1998).
[75] D. G. Truhlar, Chem. Phys. Lett. **294**, 45 (1998).
[76] M. Dallos, Th. Müller, H. Lischka, and R. Shepard, J. Chem. Phys. **114**, 746 (2001).
[77] E. Ventura, M. Dallos, and H. Lischka, J. Chem. Phys. **118**, 1702 (2003).
[78] H. Lischka, M. Dallos, P. G. Szalay, D. R. Yarkony, and R. Shepard, J. Chem. Phys. **120**, 7322 (2004).
[79] M. Dallos, H. Lischka, R. Shepard, D. R. Yarkony, and P. G. Szalay, J. Chem. Phys. **120**, 7330 (2004).